Agricultural Water Management 177 (2016) 248–263

Contents lists available at ScienceDirect

Agricultural Water Management

journal homepage: www.elsevier.com/locate/agwat

Towards modeling soil texture-specific sensitivity of wheat yield and water balance to climatic changes

Milad Nouri [a], Mehdi Homaee [a,*], Mohammad Bannayan [b], Gerrit Hoogenboom [c]

[a] Department of Soil Science, Tarbiat Modares University, P.O. Box 14115-336, Tehran, Iran
[b] Department of Agronomy, Ferdowsi University of Mashhad, P.O. Box 91775-1163, Mashhad, Iran
[c] AgWeatherNet Program, Washington State University, Prosser, WA, USA

ARTICLE INFO

Article history:
Received 24 December 2015
Received in revised form 23 July 2016
Accepted 27 July 2016

Keywords:
Crop-climate interactions
CSM-CERES-Wheat
Global warming
MarkSimGCM
Soil texture

ABSTRACT

Climate change has significant influences on agricultural water management particularly in arid and semi-arid regions. Increased water scarcity and consecutive droughts in these regions must be extensively taken into considerations in any water management scheme dealing with agricultural production. This study was aimed to find out climate changes impacts on soil water balance components and rainfed wheat yield, phenology and failure across eight different soil textural classes over 2070–2099. In order to project the future conditions, outputs of five climate models under RCP-4.5 and RCP-8.5 downscaled by MarkSimGCM were used to drive the CSM-CERES-Wheat v4.6 model. Results indicated that crop-growing season will be shorter by 10.7–21.6 days under RCP-4.5 and 25.8–45.5 days under RCP-8.5. Averaged across all investigated soils, the crop yield would decline in four studied large areas mainly due to drought and inappropriate planting date. Yield loss, averaged across all sites, are likely to be higher in finer-texture soils. More frequent harvest failure can occur over the 2080s particularly in the finer-textured soils at most studied sites. Deep drainage and runoff are expected to drop in almost all soils due to rainfall deficit. Decline of evaporation appears likely as a consequence of drought, shorter growing period and change of evapotranspiration partitioning. The crop model projected larger reduction in drainage and evaporation for coarse soils and in runoff for finer-textured soils. Higher transpiration, averaged over all sites, in coarser soils can be attributed to considerable decline of nitrogen leaching and higher subsoil water content. Furthermore, there would be an increase in soil water storage under most soil-climate simulation runs particularly in heavy-textured soils. In general, soil texture as an inherent static property highly conditions crop-climate interactions in changing climates. Furthermore, rainfed wheat production would likely be more sustainable on coarser soil textures under climate changes.

1. Introduction

Agricultural productions and food security in water-limited systems are highly impacted by water scarcity and non-water limiting factors such as poor nutrition and salinity (Rockström et al., 2010; Saadat and Homaee, 2015). In arid and semi arid regions, both water scarcity (Homaee et al., 2002a, 2002d) and salinity (Homaee et al., 2002b, 2002c; Homaee and Schmidhalter, 2008) are the two main important challenges for agricultural water management. Since pre-industrial period, rising atmospheric concentration of greenhouse gases and aerosols mainly as a result of fossil fuel overuse, land use/cover changes and agricultural activities have triggered anthropogenic global warming and climate change (CC) (IPCC, 2013). Drought exhibited upward trend since 1950 and was projected to be more severe and widespread in the future due to climatic changes, namely decreased precipitation and/or higher atmospheric evaporative demand (Dai, 2011, 2013). In the eastern Middle East including west of Iran, meteorological drought would also be more frequent and severe due to declined storm track activity (Evans, 2009). In other words, the already drought prone and water limited regions such as Iran are likely to be more liable to CC-related drought (Li et al., 2009).

The average rates of reduction in major crop yields linked to drought disaster will likely be more than 50 and 90% in 2050 and 2100, respectively, over the globe (Li et al., 2009). This drought-induced yield decrease associated with increased food demand due to westernization of diet and growing population will likely result in food insecurity in water-limited developing countries

* Corresponding author.
E-mail address: mhomaee@modares.ac.ir (M. Homaee).

http://dx.doi.org/10.1016/j.agwat.2016.07.025
0378-3774/

such as Iran (Tai et al., 2014). Therefore, it seems that more knowledge related to planning and managing water resources under climate changes is required to avoid harvest failure and food shortage in water-controlled environments. Meteorological drought and global warming would influence the components of soil water balance through affecting soil water-temperature and soil water-precipitation feedbacks (Seneviratne et al., 2010). The mathematical expression of root zone water balance can be written as (Hillel, 1998):

$$\overbrace{(P+I)}^{Gains} - \overbrace{(E+T+D+R)}^{losses} = \overbrace{\Delta S}^{Storage\ change} \quad (1)$$

$$S = \sum_{i=1}^{n} \theta_i * \Delta Z_i \quad (2)$$

where P denotes precipitation, I irrigation (included in irrigated lands), E soil evaporation, T plant transpiration, D deep downward drainage (deep percolation or leakage), R surface runoff, ΔS change in root zone water storage, θ volumetric soil moisture ($cm^3\ cm^{-3}$), Z soil horizons depth and n the number of soil layers. The components are expressed in terms of volume of water per unit soil area (i.e. equivalent depth of water) during specific time interval.

Considering heavy dependence of agricultural production on soil moisture storage particularly under rainfed condition (Bannayan et al., 2011), change of water balance is expected to greatly impact crop production under CC (Yang et al., 2015; Yang et al., 2014). Assessing climatic changes impacts on soil water balance components can therefore shed light on crop-climate interactions in the future (Eitzinger et al., 2003; Jalota et al., 2014). Soil texture also controls some ecological and hydrological processes such as water retention, aeration and nutrition availability (Hillel, 1998; Rodríguez-Iturbe and Porporato, 2005). Hence, the crop response to CC and variability is expected to vary with soil texture (He et al., 2014). Moreover, different scenarios and features of future climatic changes appear to influence crop yield differently depending on soil texture. van Ittersum et al. (2003) predicted an increase and a decline of wheat yield in a sandy soil under drier (decline of precipitation by 25%) and warmer (increase of temperature up to 3 °C) scenarios, respectively, in western Australia. On the contrary, compared with the sandy soil, the inverse changes were simulated for yield on a clay soil under above-mentioned scenarios. As a result, appropriate adaptation strategy may differ with soil types. Ludwig and Asseng (2006) concluded that wheat production on an acid sandy loam soil would likely be less vulnerable to drier and warmer climatic condition compared with a clay soil in western Australia. El Chami and Daccache (2015) also projected that climatic changes are likely to more negatively influence rainfed wheat grown on a silty clay loam (heavy-textured) soil with respect to that on a sandy loam (lighter-textured) soil in the east of England. These findings illustrate that yield response to CC will be largely impacted by soil texture. Using virtual soil profiles, Bormann (2012) found that soil texture greatly affects sensitivity of soil moisture storage changes to global warming. Yang et al. (2014) concluded that crop response to CC markedly varies with soil type. Yang et al. (2015) also studied the likely climatic changes effects on water balance components of 12 soil types under wheat in southeastern Australia. They used all soils for all surveyed sites to establish a broad range of soil types with different available water capacity. P, E and T were predicted to descend in 2021–2040 as the growth period will be shortened, while R and D would less likely be changed significantly. Further, they pointed out that spatial analyses of yield response to CC can be less uncertain and confounding if a broad range of soil types (not only a representative soil profile) are considered. The method (i.e. considering different soils for a site) used by Yang et al. (2014) can be helpful for deepening our understanding of uncertainties associated with spatial variability of soil physical properties which has been poorly addressed in the climate change literature.

To our knowledge, no research has been carried out to date to directly assess the CC influences on crop yield and water budget across a broad range of soil textures. Therefore, this study was aimed to find the CC impacts on soil water balance components, and rainfed wheat yield, growing season length and failure during the 2080s (2070–2099) relative to the baseline (1961–1990) under RCP-4.5 and RCP-8.5 over eight different textural classes in the west of Iran.

2. Materials and methods

2.1. Study area

Iran has a wide range of climatic conditions which includes 9 out of 30 climate types based on updated Köppen-Geiger climate classification (Peel et al., 2007) mainly due to the existence of the Alborz and the Zagros mountain ranges. Rain producing air masses predominantly enter from the west and northwest of Iran and cause above-average rainfall (around 300–500 mm precipitation per year) in the western half of the country owing to the Zagros mountain chain geographical location (Sadeghi et al., 2002). Consequently, semi-arid Mediterranean climate mostly dominates in the west and northwest of Iran. According to the results of some works conducted to analyze trend of precipitation (Tabari and Talaee, 2011b), temperature (Tabari et al., 2011; Tabari and Talaee, 2011a) and reference crop evapotranspiration (Talaee et al., 2014) during recent five decades, there was a shift towards drier and warmer climatic condition in Iran. The study area and location of surveyed sites are depicted in Fig. 1. Geographic and climatic characteristics of all stations are also given in Table 1.

2.2. Data

2.2.1. Climatic data

In this study, MarkSimGCM was employed to downscale coarse-scale GCMs (General Circulation Models) outputs to a $0.5^\circ \times 0.5^\circ$ latitude/longitude grid resolution using stochastic downscaling and climate typing techniques (Jones and Thornton, 2013). MarkSimGCM generates rainfall based on third-Markov stochastic model and daily temperature (minimum and maximum) as well as solar radiation using Richardson (1981) approach. The model collects the baseline period climate data (1961–1990) from the WorldClim database. In this study, an ensemble mean of five GCMs participating in the fifth phase of Coupled Model Intercomparison Project (CMIP5) (IPCC, 2013), i.e. BCC-CSM 1.1(m) (Beijing Climate Center, Climate System Model, version 1.1 (moderate resolution), $2.81^\circ \times 2.81^\circ$ latitude/longitude) (Wu, 2012), FIO-ESM (First Institute of Oceanography-Earth System Model, $2.81^\circ \times 2.81^\circ$ latitude/longitude) (Song et al., 2012), GFDL-ESM2M (Geophysical Fluid Dynamics Laboratory Earth System Model with MOM, version 4 component, $2^\circ \times 2.5^\circ$ latitude/longitude) (Dunne et al., 2012), (Institut Pierre-Simon Laplace Coupled Model, version 5A, low resolution, $1.87^\circ \times 3.75^\circ$ latitude/longitude) (Dufresne et al., 2013) and MIROC-ESM-CHEM (Model for Interdisciplinary Research on Climate, Earth System Model, Chemistry Coupled, $2.81^\circ \times 2.81^\circ$ latitude/longitude) (Watanabe et al., 2011) under RCP-4.5 and RCP-8.5 (Representative Concentration Pathways) were used for future climate condition. It should be noted that combining GCMs outputs enhances the skill, reliability and consistency of climate model forecasts (Donat et al., 2010; Tebaldi and Knutti, 2007) and reduces the bias of simulations (Fu et al., 2005). Cantelaube and Terres (2005)

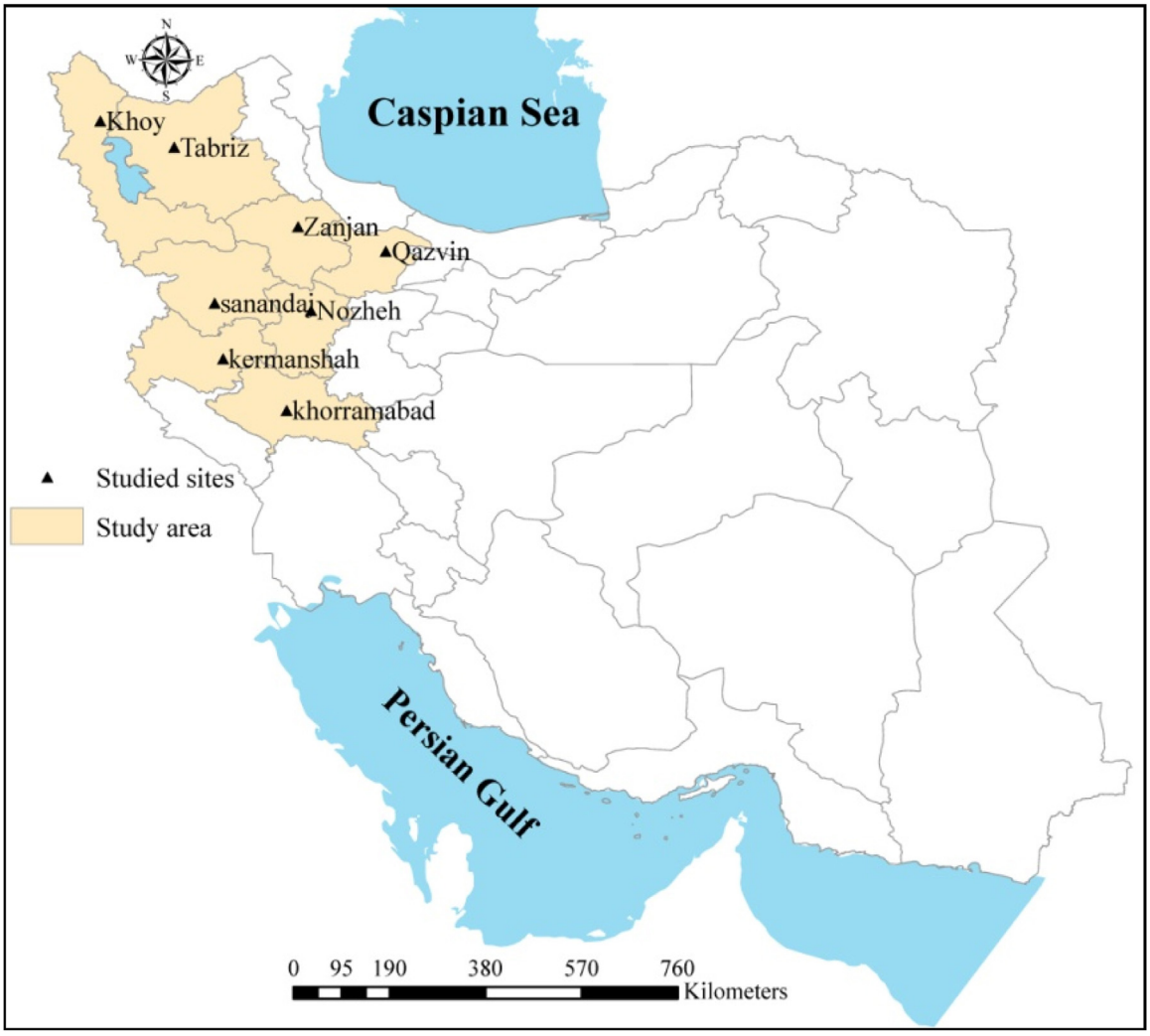

Fig. 1. Location of the study area at the west and northwest Iran.

Table 1
Some geographic characteristics and aridity index of the studied stations.

WMO[a] number	Station	Longitude	Latitude	Elevation	$\overline{AI}$[b]
		(°E)	(°N)	m.a.s.l	–
40703	Khoy	44° 58′	38° 33′	1103	0.29
40706	Tabriz	46° 17′	38° 5′	1361	0.20
40729	Zanjan	48° 29′	36° 41′	1663	0.26
40731	Qazvin	50° 3′	36° 15′	1279	0.25
40747	Sanandaj	47° 0′	35° 20′	1373	0.36
40766	Kermanshah	47° 9′	34° 21′	1318	0.32
40767	Nozheh	48° 43′	35° 12′	1680	0.23
40782	Khorramabad	48° 17′	33° 26′	1148	0.33

[a] World Meteorological Organization.
[b] Aridity index calculated based on (UNEP, 1992).

pointed out that a reliable projection of crop response to CC is obtained by using an ensemble multi-model.

Each GCM includes different models (components) for modeling physical processes related to atmoshere, aerosol, atmosphere chemistry, land surafce, ocean, ocean bio-chemistry and sea ice (Flato et al., 2013). Climate models differ in terms of structure (models), complexity, number of inclueded physical procceses and patameteres, grid resolution and vertical layers (Flato et al., 2013; Franks, 2002). Among the used GCMs, BCC-CSM 1.1(m) and FIO-ESM has the higher resolution (number of horizental grid points) for atmosphere and ocean features, respectively. Furthermore, MIROC-ESM-CHEM and IPSL-CM5A-LR are high-top atmosphere models with a fully resolved stratosphere with a model top above the stratopause (Flato et al., 2013). Flato et al. (2013) and Collins et al. (2013) have reviewed the CMIP5 GCMs in detail. The RCP-8.5 corresponds to the greatest greenhouse gases emission scenario without considering any mitigation strategy leading to a radiative forcing of 8.5 W m^{-2} at the end of the 21 st century (Riahi et al., 2011). Unkike RCP-8.5, RCP-4.5 assumes imposition of some climate mitigation policies in both energy usage and land use in order for stablizing

the radiative forcing at 4.5 W m^{-2} by 2100 (Thomson et al., 2011). In this study, the CC impact assesment was, therefore, carried out under a mitigated (RCP-4.5) and unmitigated (RCP-8.5) emission pathways.

Considering over 10000 weather stations for calibration worldwide, the model does not need to be recalibrated for each station of interest over the globe (Jones and Thornton, 2013). The model has been successfully employed in east Africa (Muluneh et al., 2014; Thornton et al., 2009), Taiwan (Tseng et al., 2015) and east India (Rao et al., 2015), which are all humid and subhumid regions. In this study, MarkSimGCM performance was evaluated by comparing model-generated and recorded data in the baseline period (1961–1990). The required historical data including minimum temperature, maximum temperature and precipitation of eight synoptic stations (Table 1) were obtained from Islamic Republic of Iran Meteorological Organization (IRIMO).

2.2.2. Soil data and soil-climate simulation runs

The soil data required to drive the soil water balance module of the CSM-CERES-Wheat are the lower limit of water availability to plants (LL, $cm^3\ cm^{-3}$, which is permanent wiling point), drained upper limit (DUL, $cm^3\ cm^{-3}$, which is field capacity), saturation (θ_s, $cm^3\ cm^{-3}$), saturated hydraulic conductivity (Ks, cm h^{-1}) and soil root growth factor (SRGF) (Ritchie, 1998). Since measuring these parameters are often tedious and time-consuming, a set of pedo-transfer functions (developed by Rawls et al. (1982) and Saxton et al. (1986)) are included in DSSAT v4.6 to predict above-mentioned soil physical properties based on some easy-to-determine soil characteristics. The readily available soil characteristics (i.e. soil texture fractions, bulk density (ρ_b) and organic carbon (OC)) collected from soil and land-use reports and maps provided by Iran soil and water research institute for the sites located in study area are given in Table 2.

In this study, eight soils (each representative for the sites listed in Table 2) mainly under rainfed wheat with different textures including sandy loam (*sl*), sandy clay loam (*scl*), loam (*l*), silt loam (*sil*), silty clay loam (*sicl*), silty clay (*sic*), clay loam (*cl*) and clay (*c*) for all sites were used under RCP-4.5 and RCP-8.5 as the soil-climate simulation runs. In this manner, soil texture roles in agrohydrological processes under CC can be assessed. Soil profile depth of all soils was 120 cm. It should be noted that this method has been recently proposed by Yang et al. (2014) and Yang et al. (2015) for addressing CC influences upon soil water budget and crop growth on a wide range of soil types. Moreover, in this study, *sl* and *scl* were classified as the coarse-textured soils (with >55% sand), *l* and *sil* as the medium-textured soils and *sicl*, *sic*, *cl* and *c* as the fine-textured soils (with >30% clay).

2.2.3. Crop data

An improved winter bread wheat cultivar (Azar-2) commonly grown under rainfed condition in west of Iran was used in this study. The data required to calibrate and evaluate the CSM-CERES-Wheat were obtained from a two-years experiment undertaken to study influences of applying different sources and rates of nitrogen fertilizer on wheat production including both quality and quantity, in three sites located in Azarbayejan-e-Sharghi (Maragheh) (37° 9′ °N, 46° 9′ °E, 1720 m.a.s.l), Kordestan (35° 12′ °N, 47° 00′ °E, 1500 m.a.s.l) and Zanjan (36° 24′ °N, 48° 17′ °E, 1662 m.a.s.l) (Feiziasl et al., 2007). The experiments were carried out employing four nitrogen rates (0, 30, 60 and 90 kg N ha^{-1}), two nitrogen fertilizer types (Urea and Ammonium nitrate) and three replications during two years (2002–2003 and 2003–2004). In Azarbayejan-e-Sharghi (Maragheh) station, two types of N-fertilizer application i.e. all-autumn and autumn-spring split were carried out. Grain yield, thousand kernel weight (TKW), days to maturity (DMA) and days to flowering (DFW) were the data used for the model calibration and evaluation. The first-year data set (including 28 sets of data) was used for calibration and the second-year data (including 28 sets of data) was considered for model evaluation. The Genotype Coefficient Calculator (Genecalc) software included in DSSAT v4.6 (Decision Support System for Agrotechnology Transfer) (Hoogenboom et al., 2014) was used to estimate the genetic coefficient values of Azar-2 cultivar depicted in Table 3. Planting method (dry seed), planting depth (5 cm), planting distribution (rows), fertilizer applications (60 kg urea-N ha^{-1}), planting date (15 October–1 November), row spacing (25 cm) and plant population at seeding (350 per m^2) were obtained based on several experiments performed in the Iranian DARI (Dryland Agricultural Research Institute) and in consulting with their researchers.

2.3. Modeling

In this study, the CSM-CERES-Wheat (Cropping System Model-Crop Environment Resource Synthesis-Wheat) (Jones et al., 2003) included in DSSAT v4.6 was used to project soil water balance components and wheat yield, failure and phenology under climatic changes. The CSM-CERES-Wheat is a field-scale, daily-scale, one dimensional, ecophysiological model which has the ability to simulate wheat growth as well as soil moisture and nitrogen budget and dynamics. Soil water balance sub-model of the CSM-CERES-Wheat is a tipping-bucket model which models water cycle and dynamics in each homogenous soil layer considering some soil physical properties introduced in the previous section. Despite not being a highly input-demanding model, the CSM-CERES-Wheat has exhibited a good performance in predicting soil water balance and dynamics particularly in cropped soils (Eitzinger et al., 2004; He et al., 2014; Kersebaum et al., 2007). Table 4 contains some climatic/hydrological processes and conditions considered in the current study.

Three types of harvest failure can be modeled with the CSM-CERES-Wheat including germination kill, winterkill and inadequate kernel (Mearns et al., 1997). In the first condition wherein the adequate water needed for germination has not been provided, crop fails 90 days after onset date. Crops may also fail to yield due to exposure to low temperature extremes during wintertime (second type of harvest failure). The third type of harvest failure occurs if modeled stem weight is appreciably low leading to less than 100 kernels per m^2. The last type seems to be triggered by soil water deficit during anthesis to beginning of grain fill (Mearns et al., 1997). In this study, all three above-explained harvest failure types were considered.

2.4. Quantitative model performance evaluation

The performance of the CSM-CERES-Wheat during the calibration and evaluation periods was assessed using three different statistics i.e. normalized root mean square error (nRMSE), means bias error (MBE) and refined Willmott's index (d_r). The mathematical expressions of these statistics are:

$$MBE = 1/n\sum_{i=1}^{n}(S_i - O_i) \tag{3}$$

$$nRMSE = \frac{100}{\overline{O}}\sqrt{(\sum_{i=1}^{n}(S_i - O_i)^2)/n} \tag{4}$$

Table 2
Some physical properties of soils, averaged over all layers, used in the study.

Soil series	Site	Tex.	sand	silt	clay	OC[1]	θ_s[2,*]	DUL[3,*]	LL[4,*]	ρ_b[5]	Ks[6,*]
			%				$cm^3\ cm^{-3}$			$g.cm^{-3}$	$cm.h^{-1}$
Osko	Tabriz	sl	61.0	24.0	15.0	0.22	0.40	0.20	0.11	1.49	2.59
Gerizeh	Sanandaj	scl	55.9	19.6	24.5	0.18	0.37	0.24	0.15	1.51	0.97
Nezamabad	Qazvin	l	42.8	37.0	20.2	0.28	0.44	0.26	0.13	1.40	1.30
Qaratapeh	Khoy	sil	20.4	54.5	25.1	0.36	0.48	0.32	0.16	1.19	0.53
Seifabad	Khorramabad	sicl	14.2	52.0	33.8	0.50	0.47	0.38	0.21	1.30	0.17
Qeidar	Zanjan	sic	10.8	44.5	44.7	0.38	0.45	0.42	0.26	1.36	0.10
Ideloo	Nozheh	cl	25.4	41.1	33.5	0.23	0.47	0.34	0.20	1.29	0.23
Amleh	Kermanshah	c	30.4	28.0	41.6	1.30	0.47	0.41	0.26	1.32	0.12

* determined based on pedo-transfer functions.
[1] Organic carbon content.
[2] Saturation.
[3] Drained upper limit.
[4] Lower limit of water availability.
[5] Soil bulk density.
[6] Saturated hydraulic conductivity.

Table 3
Genetic parameters of Azar-2 wheat cultivar.

Genetic coefficients	Description	value
P1V	Days at optimum vernalizing temperature required for completing vernalization	7
P1D	Photoperiod (pp) response (% reduction in rate/10 h drop in pp)	30
P5	Grain filling (excluding lag) phase duration (°C.d)	510
G1	Kernel number per unit canopy weight at anthesis (#/g)	11
G2	Standard kernel size under optimum conditions (mg)	36
G3	Standard, non-stressed mature tiller weight (including grain) (g dry weight)	2
PHINT	Interval between successive leaf tip appearances (°C d)	57

Table 4
Some climatic/hydrological approaches and conditions used in the study.

Process and condition	approach
Potential evapotranspiration	Priestley and Taylor (1972) equation (with modified adiabatic coefficient, α)
Potential evapotranspiration partitioning	Ritchie (1972) method
Actual evapotranspiration	Ritchie (1972) algorithm (reducing potential evaporation and transpiration based on soil water depletion rate)
Root water uptake	The limiting approach in the soil-plant-atmosphere system (Ritchie, 1981, 1998)
Runoff	Modified USDA-Soil Conservation Service curve number method (Williams et al., 1984)
Climatic variables	Precipitation, solar radiation, T_{min} and T_{max} generated and downscaled by MarkSimGCM
Drainage	Suleiman and Ritchie (2004) vertical drainage model (with modified drainage coefficient, C)
Soil moisture evaporation and redistribution	(Ritchie et al., 2009) extended two-stage model based on diffusion theory
Lower boundary condition	Free drainage and no groundwater effect
Simulation start date	30 days prior to planting date

$$d_r = \begin{cases} 1 - \{\sum_{i=1}^{n}|P_i - O_i| / c\sum_{i=1}^{n}|O_i - \bar{O}|\}, \; if \sum_{i=1}^{n}|P_i - O_i| \le c\sum_{i=1}^{n}|O_i - \bar{O}| \\ \{c\sum_{i=1}^{n}|O_i - \bar{O}| / \sum_{i=1}^{n}|P_i - O_i|\} - 1, \; if \sum_{i=1}^{n}|P_i - O_i| > c\sum_{i=1}^{n}|O_i - \bar{O}| \end{cases} \quad (5)$$

where S_i is the simulated values, O_i is the observed values, $\bar{O}$ is mean of the observations, c equals to 2 and n is the number of time steps.

The normalized root mean square error (nRMSE) is frequently used to characterize the differences between the simulated and recorded values in the agrohydrology literature (Homaee et al., 2002a). The model performance is considered perfect with nRMSE value less than 10%, good if nRMSE is between 10% and 20%, fair if nRMSE is between 20% and 30% and poor if nRMSE quantity is greater than 30% (Dettori et al., 2011). MBE is an index quantifying model bias and systematic error and its negative (positive) values indicate model tendency to underestimate (overestimate) (Palosuo et al., 2011). d_r is a dimensionless relative error or goodness-of-fit measure varying between −1 and 1(Willmott et al., 2012). If the simulated values are equivalent to the observations ($S_i = O_i$), the model performance is excellent and the magnitude of d_r statistic is one and the quantity of MBE and nRMSE statistics are equal to zero.

3. Results and discussions

3.1. Models evaluation

3.1.1. MarkSimGCM

The results listed in Tables 5–7 show that MarkSimGCM adequately well synthesized T_{min}, T_{max} and precipitation time series for the baseline period (1961–1990). Despite the significant differences between modeled and observed T_{min} at Nozheh and Tabriz (Table 5), and T_{max} at Zanjan site during some seasons (Table 6), MarkSimGCM performed acceptably well in generating T_{min} and T_{max} time series over 1961–1990. The model slightly tended to overestimate rainfall amount on seasonal and annual scales for the majority of the study sites (Table 7). In addition, it seems that in case of predicting summertime precipitation, model performance was poor compared with that in other seasons. Overall, the model seems to be capable of adequately simulating growing season climatic variables required to run the CSM-CERES-Wheat.

3.1.2. The CSM-CERES-Wheat

The CSM-CERES-Wheat showed a good estimate of grain yield considering nRMSE values (between 10 and 20%) in both calibration and testing period (Table 8). Further, the simulation accuracy of the

Table 5
Comparison of modeled (Mod.) with recorded (Rec.) seasonal and annual average T_{min} data over 1961–1990.

Site	Variable	Winter (DJF[a])		Spring (MAM[b])		Summer (JJA[c])		Autumn (SON[d])		Annual	
		Rec.	Mod.	Rec.	Mod.	Rec.	Mod.	Rec.	Mod.	Rec.	Mod.
Khoy	Mean	−5.1	−4.1	5.0	4.6	14.6	15.8*	5.6	5.8	5.0	5.6
	Variance	9.4	11.8	1.6	1.8	1.6	0.7	1.9	1.8	2.0	1.3
Tabriz	Mean	−4.8	−4.5	6.0	4.8*	18.0	15.9*	8.2	8.0	6.8	6.1*
	Variance	5.3	6.1	4.8	6.9	0.7	0.7	0.6	0.8	0.6	0.3
Zanjan	Mean	−6.4	−5.9	3.4	3.0	13.4	12.9	5.3	5.4	3.9	3.8
	Variance	8.1	10.0	1.0	1.0	1.0	0.8	0.7	0.9	1.0	1.3
Nozheh	Mean	−5.1	−4.1	5.0	5.6	14.6	15.8*	5.6	6.7*	5.0	6.1*
	Variance	9.4	10.8	1.6	0.8	1.6	0.7	1.9	0.8	2.0	0.3
Qazvin	Mean	−3.2	−2.8	6.2	6.1	16.4	16.3	7.9	7.9	6.8	6.9
	Variance	5.2	2.3	1.2	0.8	1.3	0.6	1.5	1.8	1.1	1.4
Khorramabad	Mean	1.0	1.1	8.2	8.2	17.8	18.4	9.8	10.2	9.2	9.5
	Variance	3.3	4.6	2.7	1.7	4.1	4.5	3.5	4.7	2.8	3.2
Sanandaj	Mean	−4.7	−4.5	4.3	4.3	15.2	15.0	5.8	5.7	5.1	5.2
	Variance	6.1	7.2	1.2	1.0	1.3	0.7	1.1	0.9	1.5	1.3
Kermanshah	Mean	−2.8	−2.9	4.9	5.1	14.4	14.4	6.3	5.9	5.7	5.7
	Variance	3.2	3.9	0.9	0.9	1.0	0.7	1.2	0.9	0.7	0.6

* Significant difference at the level of 95%.
[a] December-January-February.
[b] May-April-March.
[c] June-July-August.
[d] September-October-November.

Table 6
Comparison of modeled (Mod.) with recorded (Rec.) seasonal and annual average T_{max} data over 1961–1990.

Site	Variable	Winter (DJF[a])		Spring (MAM[b])		Summer (JJA[c])		Autumn (SON[d])		Annual	
		Rec.	Mod.	Rec.	Mod.	Rec.	Mod.	Rec.	Mod.	Rec.	Mod.
Khoy	Mean	4.0	4.8	17.6	17.8	31.2	31.7	20.4	20.5	18.3	18.8
	Variance	7.5	8.6	2.3	1.8	1.8	1.5	1.4	0.5	1.5	1.2
Tabriz	Mean	2.9	2.2	16.5	16.2	31.3	30.7	20.1	19.7	17.8	17.2
	Variance	1.0	1.6	1.3	0.9	1.1	0.6	1.2	0.7	0.8	0.7
Zanjan	Mean	3.9	5.1*	16.7	15.9*	30.9	30.3	20.3	20.6	18.0	18.0
	Variance	6.9	8.5	1.5	0.9	0.8	0.5	1.4	0.6	0.9	0.6
Nozheh	Mean	4.0	4.8	17.6	17.8	31.2	31.7	20.4	20.5	18.3	18.8
	Variance	7.5	7.6	2.3	1.8	1.8	1.5	1.4	1.5	1.5	1.2
Qazvin	Mean	8.9	8.4	19.8	19.8	34.1	33.8	23.1	23.4	21.5	21.4
	Variance	8.3	6.5	2.2	1.9	0.6	0.4	2.1	1.5	1.5	1.2
Khorramabad	Mean	12.4	12.4	23.0	22.1	38.2	38.4	27.5	27.7	25.3	25.2
	Variance	3.2	3.1	1.7	2.8	1.0	1.3	1.3	1.4	1.0	1.1
Sanandaj	Mean	6.7	6.1	19.2	18.3	35.1	34.5	23.7	22.4	21.2	20.3
	Variance	6.6	10.4	1.5	0.9	0.8	0.5	0.9	0.5	0.8	0.9
Kermanshah	Mean	8.4	9.0	19.9	18.8*	36.1	35.5	24.8	24.2	22.3	21.9
	Variance	4.8	4.1	1.1	0.9	0.7	1.0	0.9	0.5	0.6	0.1

* Significant difference at the level of 95%.
[a] December-January-February.
[b] May-April-March.
[c] June-July-August.
[d] September-October-November.

model was excellent (nRMSE < 10%) for days to maturity (DMA) and days to flowering (DFW) during both phases and for thousand kernel weight (TKW) over the calibration period. Given MBE values, the model often tended to underestimate grain yield and TKW and overestimate DMA and DFW. Furthermore, quantities of close to 0.5 for d_r illustrated that sum of the error-magnitudes was approximately one half of the sum of perfect modeled and recorded grain yield, DMA and DFW deviations (Willmott et al., 2012). In the testing phase, as the value of absolute error indicated good estimation of TKW (10% < nRMSE < 20%), low value of d_r for TKW can be due to low variation of recorded data (Willmott et al., 2012).

3.2. Future changes in climate

The NDJ (November-December-January, sowing to terminal spikelet initiation) and MAM (March-April-May, beginning of ear growth to end of grain filling) are the most critical periods for winter crop development in the study area (Table 9). Any changes in climatic variables during these periods can therefore greatly impact wheat yield. Averaged across all sites, an increase of 2.3 and 4.8 °C in annual T_{min} and 2.9 and 5.6 °C in annual T_{max} were projected under RCP-4.5 and RCP-8.5, respectively (Table 9). In addition, temperature increment will be larger during MAM compared with that in

Table 7
Comparison of simulated (Mod.) with recorded (Rec.) seasonal and annual average precipitation data over 1961–1990.

Site	Variable	Winter (DJF[a])		Spring (MAM[b])		Summer (JJA[c])		Autumn (SON[d])		Annual	
		Rec.	Mod.	Rec.	Mod.	Rec.	Mod.	Rec.	Mod.	Rec.	Mod.
Khoy	Mean	67.2	71.2	144.2	144.6	41.2	28.4	63.9	66.7	316.2	310.9
	Variance	436.0	323.2	2443.9	2963.2	898.2	421.8	1732.4	2051.9	7478.0	7741.5
Tabriz	Mean	77.7	83.2	138.7	151.3	26.1	32.0	64.4	79.4	306.5	345.9
	Variance	1076.6	1473.6	3892.1	4290.5	482.7	595.6	1659.8	2343.0	8106.3	8561.8
Zanjan	Mean	94.6	126.3*	148.1	160.3	15.1	7.5*	58.2	55.5	316.0	349.6
	Variance	739.9	2299.4	2509.8	2100.3	155.2	94.7	1293.2	1661.0	7142.4	7782.7
Nozheh	Mean	67.2	71.2	144.2	144.6	41.2	28.4	63.9	66.7	316.2	310.9
	Variance	436.0	1323.2	2443.9	2963.2	898.2	421.8	1732.4	2051.9	7478.0	7817.3
Qazvin	Mean	130.9	105.3	128.6	168.4	8.7	11.1	49.0	60.9	317.3	344.7
	Variance	1702.6	2085.0	2320.9	2743.1	59.7	135.6	1466.5	2020.1	8014.4	7098.8
Khorramabad	Mean	242.1	231.7	188.8	184.2	0.6	9.7*	77.7	94.3	509.2	519.9
	Variance	5318.6	5135.9	6077.1	4977.5	1.3	12.4	2289.3	2518.8	14297.4	15641.1
Sanandaj	Mean	199.4	215.3	199.9	230.2	2.9	12.8*	86.2	82.5	488.4	540.4
	Variance	3588.6	4116.2	4391.2	5639.6	22.3	42.9	2884.3	1903.9	14818.5	12006.0
Kermanshah	Mean	202.0	210.5	189.3	202.5	1.0	14.5*	84.5	88.3	477.6	515.8
	Variance	3242.5	3916.8	7246.9	7859.7	4.6	23.4	2832.0	2623.9	15156.5	14782.7

* Significant difference at the level of 95%.
[a] December-January-February.
[b] May-April-March.
[c] June-July-August.
[d] September-October-November.

Table 8
The obtained statistics for evaluating the CSM-CERES-Wheat performance.

Variable	Set of data	nRMSE[a] (%)	MBE[b],*	d_r[c] (−)
Grain yield	Calibration	14.3	−76.7	0.64
	Validation	16.4	−170.8	0.55
TKW[d]	Calibration	7.0	−0.9	0.41
	Validation	10.1	−3.5	0. 16
DMA[e]	Calibration	4.0	3.0	0.49
	Validation	7.6	1.9	0.48
DFW[f]	Calibration	3.5	2.4	0.68
	Validation	7.9	3.2	0.47

* MBE units for Grain yield, TKW, DMA and DFW are kg, g, day and day, respectively.
[a] Normalized root mean square.
[b] Mean bias error.
[c] Refined Willmott's index.
[d] Total kernel weight.
[e] Days to maturity.
[f] Days to flowering.

NDJ at most of the stations. The west and northwest parts of Iran would receive lower precipitation and probably experience more droughts and low rainfall years (Table 9). The early growing season (NDJ) precipitation was projected to decrease by >15% in Khoy, Tabriz, Qazvin and Khorramabad under both RCPs. These results are consistent with those already reported by Evans (2009), Chenoweth et al. (2011) and Lelieveld et al. (2012) who predicted a serious rainfall shortage in northwest and west Iran through the 21 st century. Furthermore, similar results have also been projected for future climatic condition of northeastern Iran by Bannayan and Eyshi Rezaei (2014) and Eyshi Rezaie and Bannayan (2012).

3.3. Projection of crop related variables

3.3.1. Length of growing season

Wheat growing season length would presumably be curtailed in the future with respect to the baseline period (1961–1990) (Fig. 2a) as a consequence of temperature rise (Table 9). Averaged over all soils, decrease of growing season length (day) ranged from 10.2 (in Qazvin) to 24.4 (in Tabriz) under RCP-4.5 and from 15.3 (in Nozheh) to 43.3 (in Kermanshah) under RCP-8.5. Influencing grain filling duration and photosynthetic processes, curtailed growing season length would affect wheat production in terms of both quality and quantity (Hatfield et al., 2011).

3.3.2. Wheat grain yield

Wheat yield is likely to increase in Sanandaj, Nozheh and Kermanshah (under RCP-4.5) and decrease in Khoy, Tabriz, Zanjan (under RCP-4.5), Khorramabad and Qazvin under most of the soil-climate simulation runs (Fig. 2b). Averaged across all soils, change in yield (kg ha^{-1}) would be +304.9 and +381.8 in Sanandaj, +93.0 and +78.4 in Nozheh, −139.6 and −362.7 in Khoy, −96.8 and −168.3 in Tabriz, +312.6 and −58.0 in Kermanshah, −54.0 and +57.2 in Zanjan, −12.7 and −80.4 in Qazvin, and −227.6 and −314.7 in Khorramabad under RCP-4.5 and RCP-8.5, respectively (Fig. 2b). The greatest yield loss was projected in Khorramabad and Khoy under RCP-4.5 and RCP-8.5, respectively. Therefore, Khorramabad and Khoy appear to be the most sensitive sites to CC in the last 30-yr of the 21 st century.

Table 9
Average of annual, NDJ (November-December-January) and MAM (March-April-May) T_{min}, T_{max} and precipitation (P) (ensemble average of the GCMs) during 1961–1990 and changes of the variables (T_{min}, T_{max} (ΔC°) and P (Δ %)) in the 2080 s relative to the baseline period under the RCPs.

Site	Baseline (1961–1990)								
	T_{min} (C°)			T_{max} (C°)			P (mm)		
	Ann.	NDJ	MAM	Ann.	NDJ	MAM	Ann.	NDJ	MAM
Khoy	5.6	−2.3	4.6	18.8	7.1	17.8	310.9	76.9	144.6
Tabriz	6.1	−3.1	4.8	17.2	5.9	16.2	345.9	94.5	151.2
Zanjan	3.8	−5.0	3.0	18.0	6.1	15.9	349.6	105.6	160.3
Nozheh	6.1	−3.6	5.6	18.8	6.9	17.8	310.8	80.9	144.6
Qazvin	6.9	−0.9	6.1	21.4	10.6	19.8	344.7	107.3	168.4
Khorramabad	9.5	2.5	8.2	25.2	14.4	22.1	519.9	230.3	184.2
Sanandaj	5.2	−3.0	4.3	20.3	9.6	18.3	540.4	204.9	230.1
Kermanshah	5.7	−1.4	5.1	21.9	10.6	18.9	515.8	209.9	202.5
	2080s (RCP-4.5)								
Khoy	2.45	2.0	2.0	3.0	2.4	2.7	−12.4	−16.9	−7.6
Tabriz	2.4	1.9	2.0	2.9	2.3	2.6	−10.4	−18.3	−0.3
Zanjan	2.2	1.8	1.9	2.7	2.3	2.5	−6.7	−16.6	−5.6
Nozheh	2.3	1.9	2.0	2.9	2.5	2.8	−7.4	−0.6	−9.0
Qazvin	2.1	2.0	1.6	2.6	2.1	2.7	−14.4	−16.8	−17.6
Khorramabad	2.4	2.0	2.1	2.9	2.7	2.7	−3.7	−26.6	−4.8
Sanandaj	2.4	1.8	2.2	3.0	2.4	3.0	−7.4	−2.3	−7.5
Kermanshah	2.3	1.9	2.1	2.9	2.6	2.8	−11.1	−4.8	−16.1
	2080s (RCP-8.5)								
Khoy	4.9	4.2	4.0	5.8	5.1	5.3	−24.1	−39.8	−23.6
Tabriz	4.7	3.9	4.1	5.6	4.7	5.3	−11.6	−19.9	0.7
Zanjan	4.5	3.7	4.0	5.3	4.5	5.2	−7.4	−2.9	−10.1
Nozheh	4.8	4.0	4.4	5.6	4.9	5.6	−2.5	−1.9	−2.2
Qazvin	4.4	3.6	4.0	5.2	4.4	5.1	−8.7	−15.8	−10.2
Khorramabad	5.2	4.4	4.8	5.7	5.2	5.6	−9.3	−24.1	−8.1
Sanandaj	5.0	4.1	4.5	5.7	5.1	5.6	−13.0	−5.8	−12.4
Kermanshah	5.1	4.4	4.5	5.8	5.4	5.5	−15.6	−23.1	−15.4

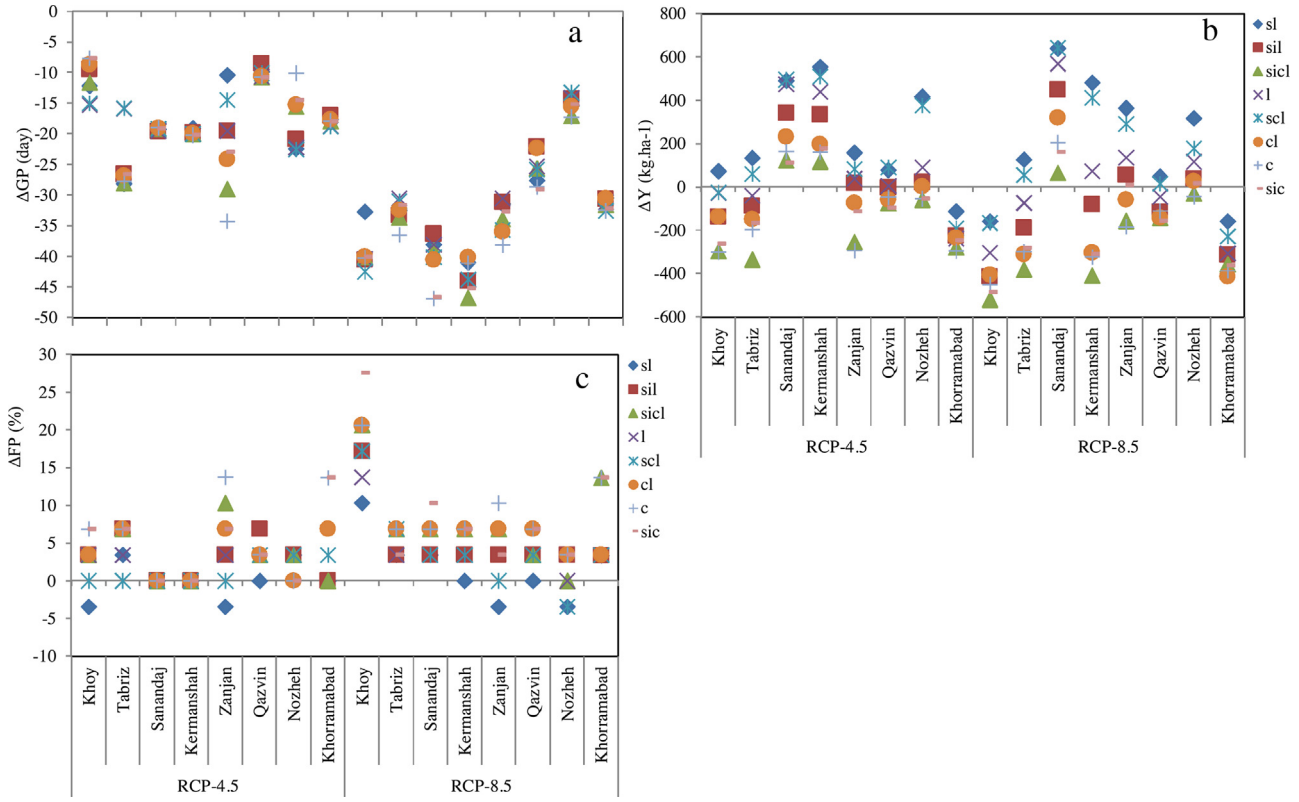

Fig. 2. Absolute changes in wheat growth period (ΔGP) (day), yield (ΔY) (kg ha^{-1}) and failure probability (ΔFP) (%) under RCP-4.5 and RCP-8.5 over eight classes of soil texture in the 2080s with respect to the baseline period.

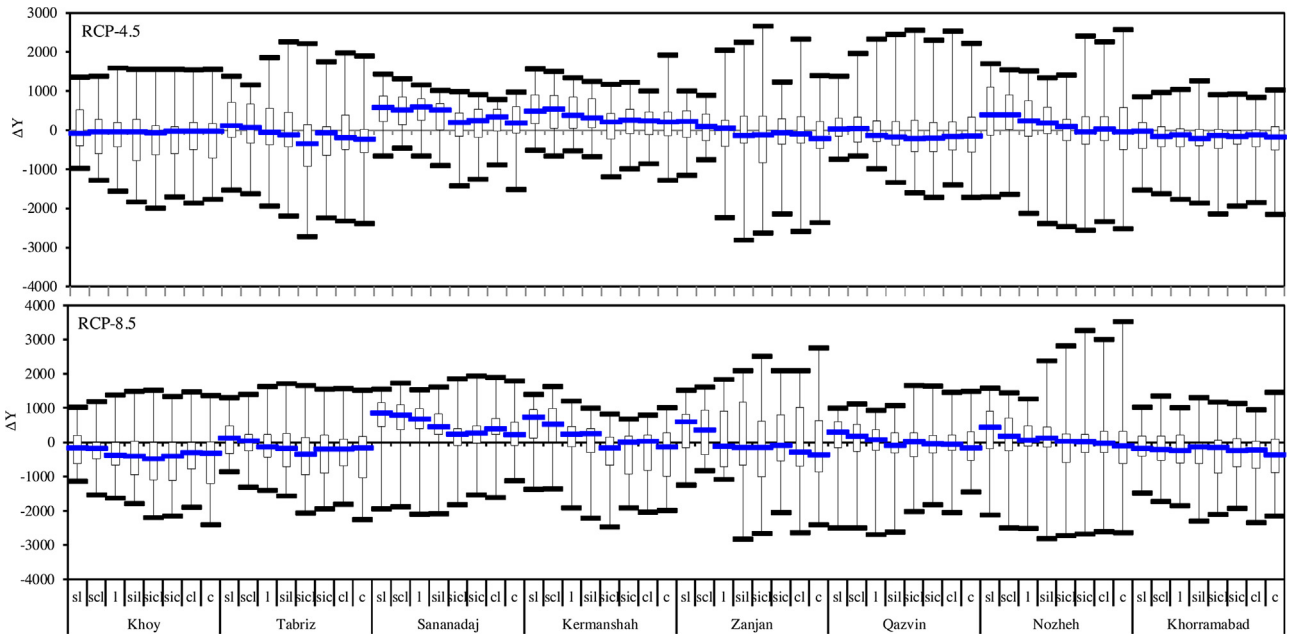

Fig. 3. The box plots of grain yield changes (kg ha^{-1}) along eight soil textures and sites in the 2080s relative to the baseline period (boxes boundaries indicate the 25th and 75th percentiles, the lines within the boxes mark the median and the inner and outer fences represent the lowest and highest values, respectively).

The NDJ rainfall shortage (>15%) seems to be the main cause of wheat yield loss in Khoy, Khorramabad, Tabriz, Qazvin, Kermanshah (under RCP-8.5) and Zanjan (under RCP-4.5) (Table 9). In Khorramabad, as the warmest and most sensitive region under RCP-4.5, decreased rainfall and temperature rise are likely to result in a higher harvest loss. As in some locations such as Khorramabad and Tabriz wherein yield loss would be highly likely, the MAM rainfall will not considerably decrease but the early season rainfall (NDJ) in the future, the MAM precipitation appears not to be of same importance as the early season precipitation (NDJ). In some sites such as Sanandaj and Nozheh, as a severe early season drought is not anticipated, crop yield was modeled to increase, averaged over all soils, due to temperature rise and CO_2 enrichment.

The projected wheat yield varies greatly over the soils and sites (Fig. 3). The interquartile ranges (IQR) of yield changes, averaged over all soils, were 805.2 and 891.9, 877.6 and 978.1, 642.5 and 594.0, 695.3 and 915.0, 744.6 and 1393.6, 672.0 and 654.8, 741.5 and 766.8, and 490.1 and 782.3 kg ha^{-1} for Khoy, Tabriz, Sanandaj, Kermanshah, Zanjan, Qazvin, Nozheh and Khorramabad under RCP-4.5 and RCP-8.5, respectively.

We considered two sites i.e. Khoy (a northern site) and Kermanshah (a wetter southern site) to better explain the impacts of CC on wheat yield across all eight textures under RCP-8.5. The changes in grain yield were −158.3, −165.2, −302.9, −413.8, −519.6, −485.8, −405.8 and −450.1 (kg ha^{-1}) in Khoy and +480.5, +413.9, +74.2, −80.9, −408.2, −310.6, −303.5 and −322.7 (kg ha^{-1}) in Kermanshah under RCP-8.5 for *sl*, *scl*, *l*, *sil*, *sicl*, *sic*, *cl* and *c*, respectively. For *sl* and *scl*, an increase of grain yield in Kermanshah and a lower decrease of yield in Khoy was projected. A higher reduction in grain yield is expected to occur in both sites in the heavier-textured soils (i.e. *sicl*, *sic*, *cl* and *c*). Thus, it appears that CC will cause a greater yield loss in the heavier-textured soils (i.e. *sic*, *sicl*, *cl* and *c*) than in the light-textured soils (i.e. *sl* and *scl*). In other stations, similar results were obtained (Fig. 2b). Averaged over all sites, the model projected the highest enhancement (kg ha^{-1}) of wheat yield in *sl* by 224.7 and 208.0 under RCP-4.5 and RCP-8.5, respectively. The greatest yield loss, averaged across all sites, were 132.2 and 240.6 (kg ha^{-1}) predicted in *sicl* under RCP-4.5 and RCP-8.5, respectively. Except in Khorramabad and Khoy (under RCP-8.5), there was a projection of increase in *sl* and *scl*. Accordingly, wheat cropped over the sandy soils seems to be less sensitive to CC.

The IQR values, averaged over all sites, ranged between 653.0 (for *sl*) and 767.3 (for *sicl*) under RCP-4.5 and 801.1 (for *scl*) and 1080.4 (for *c*) kg ha^{-1} under RCP-8.5. In general, there is a larger variation of yield change over the clay soils compared with sandy soils (Fig. 3).

3.3.3. Wheat failure

The results (Fig. 2c) revealed that harvest failure would be more frequent in most of the sites as a result of meteorological drought and inappropriate sowing date in 2070–2099. More frequent below-normal rainfall years will enhance the probability of first and third types of harvest failure. Furthermore, averaged across all soil textures, the change range of harvest failure probability (%) was from 0 (in Sanandaj and Kermanshah) to 5.2 (in Khorramabad and Tabriz, Zanjan) under RCP-4.5 and 0.86 (in Nozheh) to 18.5 (in Khoy) under RCP-8.5. Averaged across all sites, harvest failure is anticipated to change (%) between 0.0 (in *sl*) and +5.6 (in *c*) under RCP-4.5 and +1.7 (in *sl*) and +9.5 (in *sic* and *c*) under RCP-8.5. Regarding the substantial contribution of heavy-textured soils in the western half of Iran towards producing rainfed agricultural production, serious attention should be paid in adopting appropriate adaptive measures to avoid crop failure in such soils. It should be noted that in Khoy and Khorramabad, as the most sensitive sites, crop failure probability would significantly enhance in the late 21st century.

3.4. Projection of the soil water balance components

3.4.1. Precipitation

In general, a decline in growing season precipitation, as the primary driver of the hydrological cycle, was foreseen under most of the soil-climate simulation runs by 2100 over the study area (Fig. 4a). Precipitation, averaged over all soils, was predicted to change (mm d^{-1}) in the range of −0.16 (in Khoy) to −0.02 (in Sanandaj) under RCP-4.5 and −0.44 (in Khoy) to +0.024 (in Nozheh) under RCP-8.5. The largest IQR of precipitation change was found

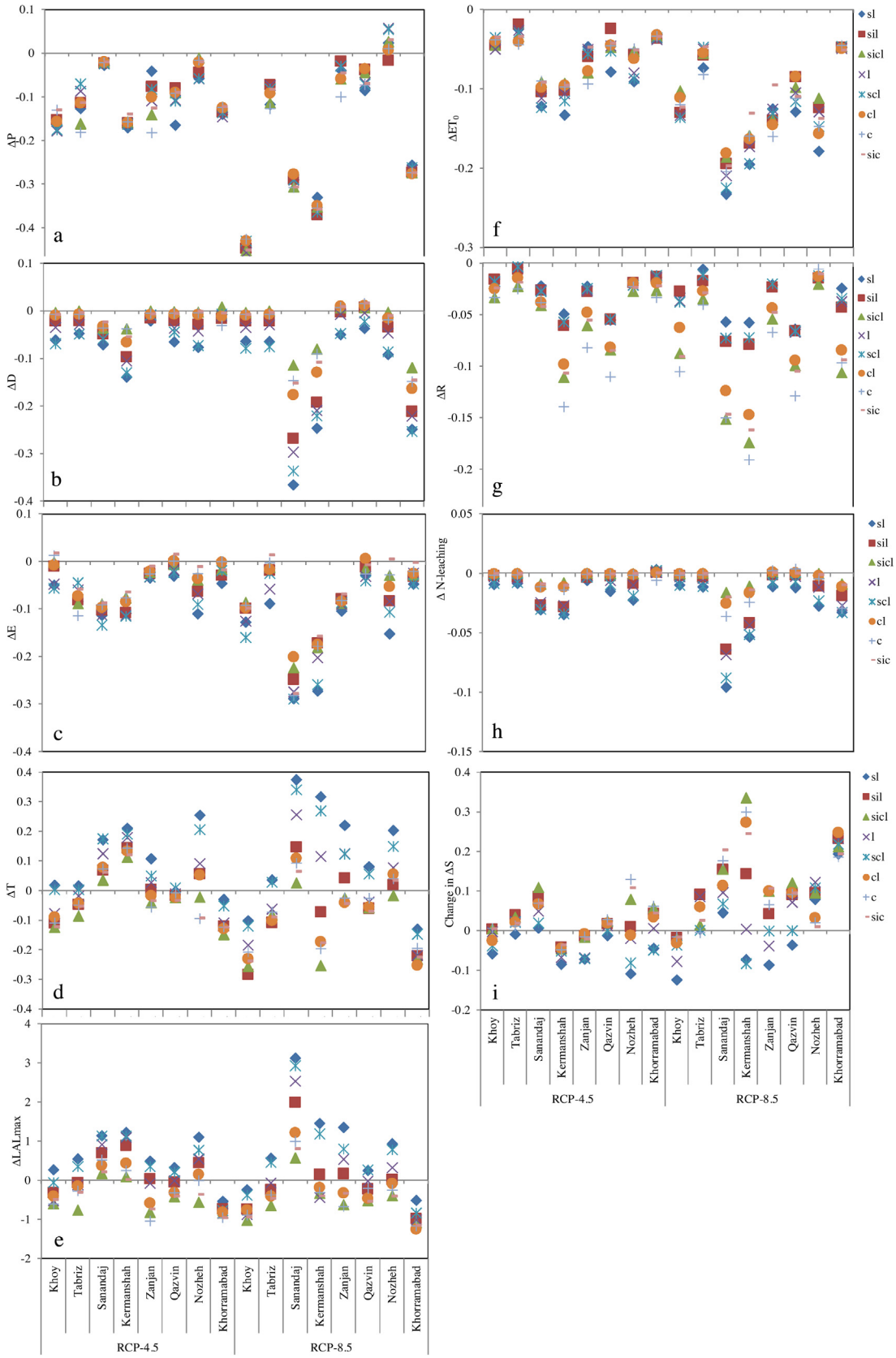

Fig. 4. Daily absolute changes in precipitation (ΔP) (mm d^{-1}), deep drainage (ΔD) (mm d^{-1}), evaporation (ΔE) (mm d^{-1}), transpiration (ΔT) (mm d^{-1}), maximum LAI (ΔLAImax) (m^2 m^{-2}), potential evapotranspiration (ΔET_0) mm d^{-1}), runoff (ΔR) (mm d^{-1}), soil water storage (ΔS) (mm d^{-1}) and N-leaching (ΔN-leaching) (Kg ha^{-1} d^{-1}) during wheat-growing season under RCP-4.5 and RCP-8.5 over eight classes of soil texture in the 2080s with respect to the baseline period.

for Khorramabad (1.2 mm d^{-1}) under RCP-4.5 and Kermanshah (1.1 mm d^{-1}) under RCP-8.5 (Fig. 5a and b).

3.4.2. Deep drainage and N-leaching

In case of deep drainage (D), the model projected percolation loss decreases mainly due to rainfall shortage (Fig. 4b). Averaged over all sites, *sl* showed the greatest reductions of deep drainage (by 0.060 and 0.15 mm d^{-1} under RCP-4.5 and RCP-8.5, respectively) as drainage is a significant portion of the light-textured soils water budget (Asseng et al., 2000). Spatially, larger decreases in drainage, averaged over all soils, are anticipated for Kermanshah by 0.083 and 0.16, Khorramabad by 0.01 and 0.19 and Sanandaj by 0.045 and 0.23 mm d^{-1} under RCP-4.5 and RCP-8.5, respectively, since percolation is of major importance in the above 450 mm rainfall regions (Asseng et al., 2000). Rainfall deficit would therefore yield a larger decline in deep percolation in the wetter locations and sandier soils.

In addition, averaged across all sites, IQR of ΔD changed in range of 0.30 (for *sl*) to 0.03 (for *sicl*) under RCP-4.5 and 0.25 (for *sl*) to 0.039 (for *sicl*) mm d^{-1} under RCP-8.5 (Fig. 5c and d). Variation of drainage change (Fig. 5c and d) was more prominent in the coarse-textured soils (i.e. *sl* and *scl*) and wetter sites (i.e. Sanandaj, Khorramabad and Kermanshah).

As can be seen from Fig. 4h, the greatest decrease in N-leaching, averaged over all sites, was simulated in *sl* (0.015 and 0.032 kg ha^{-1} d^{-1} for RCP-4.5 and RCP-8.5) followed by *scl* (0.014 and 0.029 for RCP-4.5 and RCP-8.5). In addition, the highest decline of N-leaching (kg ha^{-1} d^{-1}), averaged over all soils, was 0.021 at Kermanshah followed by 0.019 at Sanandaj under RCP-4.5 and 0.052 at Sanandaj followed by 0.032 at Kermanshah under RCP-8.5. In those stations with higher precipitation, the higher reduction in N-leaching is, therefore, expected to occur. Decline of nitrogen leaching beyond the root zone due to decreased vertical percola-

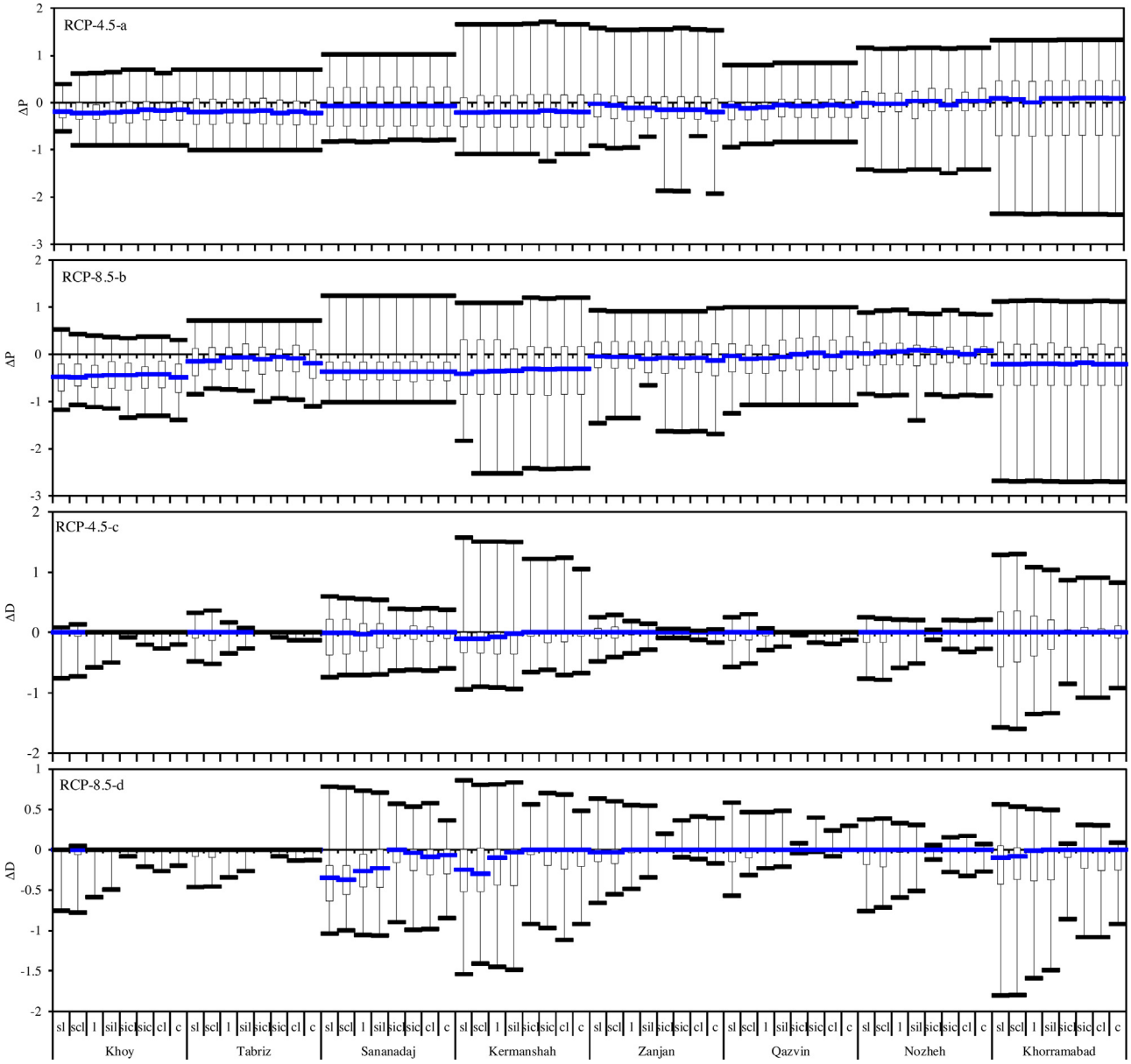

Fig. 5. The box plots of changes in precipitation (ΔP), drainage (ΔD), evaporation (ΔE), transpiration (ΔT), runoff (ΔR) and soil water storage (ΔS) mm d^{-1}) along eight soil textures and sites under RCP-4.5 and RCP-8.5 in the 2080 s relative to the baseline period (boxes boundaries indicate the 25th and 75th percentiles, the lines within the boxes mark the median and the inner and outer fences represent the lowest and highest values, respectively).

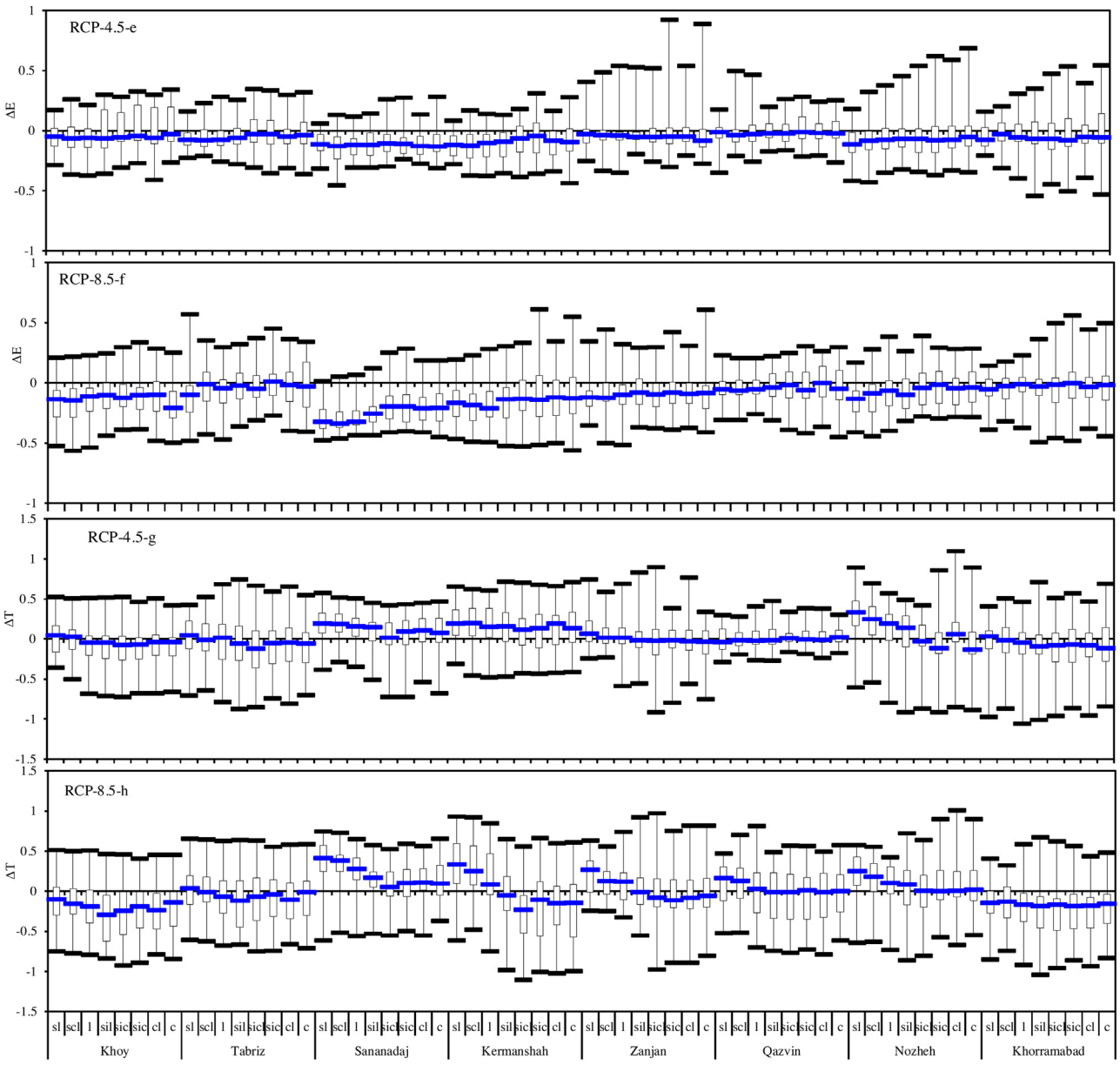

Fig. 5. (*Continued*)

tion can benefit crop growth particularly in coarse-texture soils (van Ittersum et al., 2003).

3.4.3. Evapotranspiration

There will be a reduction of soil evaporation (E) ranging from −0.008 (in Qazvin) to −0.103 (in Sanandaj) under RCP-4.5 and from −0.019 (in Qazvin) to −0.260 (in Sanandaj) mm d^{-1} under RCP-8.5 averaged across all soils in the 2080s (Fig. 4c). Reduction of evaporation can be due to the shortened length of growth season, changed evapotranspiration partitioning and CC-induced soil water deficit over the study area.

Averaged over all soils, transpiration (T) was predicted to be reduced in Tabriz, Khoy, Khorramabad and Qazvin, and enhanced in Zanjan, Kermanshah (under RCP-4.5), Nozheh and Sanandaj (Fig. 4d). The rise of crop transpiration loss can be related to increased root (Tubiello et al., 1995) and above-ground (maximum leaf area index (LAI_{max}), Fig. 4e) (Ferretti et al., 2003) biomass as a consequence of insignificant changes of NDJ rainfall, CO_2 fertilization and higher nutrient availability due to reduced deep drainage. However, decreased T in some sites such as Khoy, Khorramabad and Qazvin can be explained by drought (particularly during NDJ period) and inappropriate planting date. Considering the close relationship existing between T and crop yield, it is not surprising that changes of T are comparable to those of wheat yield (Fig. 2b).

Averaged across all sites, evaporation decline (mm d^{-1}) ranged from 0.027 (in *sic*) to 0.072 (in *sl*) under RCP-4.5 and from 0.07 (in *sic*) to 0.14 (in *sl*) under RCP-8.5. In addition, the range of projected changes of transpiration (mm d^{-1}), averaged across all sites, was from −0.033 (in *sic*) to +0.094 (in *sl*) under RCP-4.5 and from −0.097 (in *sic*) to +0.126 (in *sl*) under RCP-8.5. As a result, one can express that changes in E and T have a great sensitivity to soil texture. In coarse-textured soils, rainfall mainly infiltrates deeper into soil due to their high infiltration rate and near-saturated hydraulic conductivity avoiding high level of soil moisture evaporation loss (Fernandez-Illescas et al., 2001). However, less rain water infiltrates to deeper horizons in heavier-texture soils particularly in water-limited regions which may raise the risk of terminal drought (Lane et al., 1998; Ludwig and Asseng, 2006). Furthermore, lower

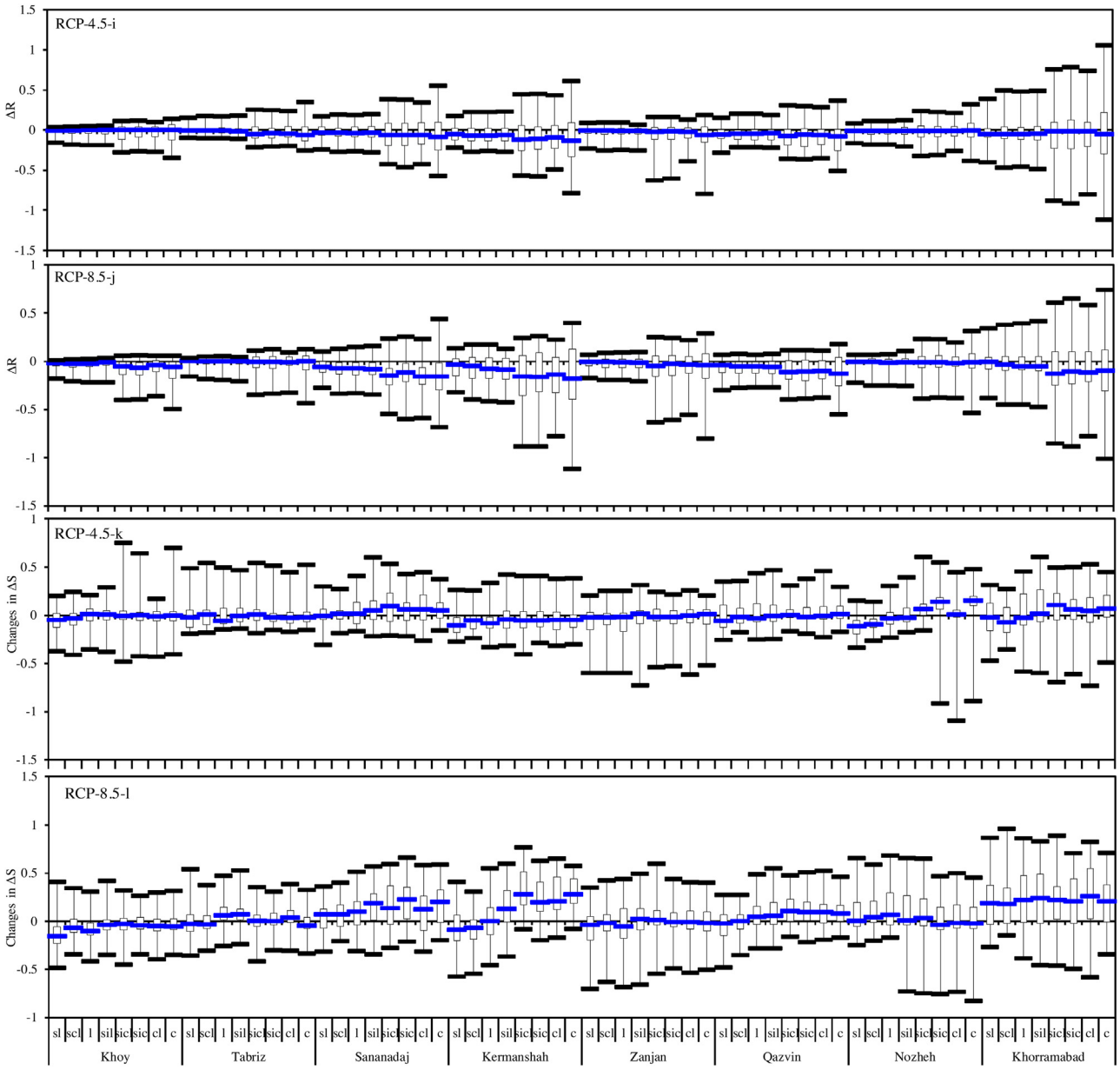

Fig. 5. (*Continued*)

water retention capacity and desorptivity of light-texture soils limit the upward evaporation flux from underlying layers to the evaporating surface by capillary forces resulting in more deeply stored transpirable water (Hillel, 1998; Ritchie, 1972). In contrast, a considerable quantity of water retained in the topsoil nonproductively evaporates from the exposed surface of those soils having appreciable amount of clay (>30%) (Lane et al., 1998). Thus, the results exhibited less reduction in evaporation loss in the fine-textured soils than the coarser-textured ones (i.e. *sl* and *scl*) (Fig. 4c). Furthermore, more frequent harvest failure can be another explanation for a higher reduction of transpiration in the finer-textured soils. It should be noted that a lower transpiration to evaporation ratio during the growing season is expected when crop fails. In addition, a larger decline of deep drainage projected in the sandier soils (e.g. *sl* and *scl*) (Fig. 4b) would cause a greater reduction of N-leaching loss in such soils (Fig. 4h). Diminished N-leaching (Fig. 4h), hence, appears likely to result in higher root nitrogen uptake, LAI (Fig. 4e) and transpiration in *sl* and *scl* (Fig. 4d), whereas nitrate does not significantly leach downward from the root zone of heavy-textured soils in water-limited regions (Fig. 4h). As a consequence, one can conclude that wheat growing on the coarse-textured soils (e.g. *sl* and *scl*) would likely benefit from elevated CO_2 and temperature due to less water stress and more nutrient availability in most of the sites (Fig. 2b).

Averaged over all sites, the IQR of ΔE was in range of 0.14 (for *sl*) to 0.20 (for *sic*) under RCP-4.5 and 0.17 (for *sl*) to 0.25 (for *c*) mm d^{-1} under RCP-8.5 (Fig. 5e and f). Moreover, the IQR of ΔT changed from 0.27 (for *scl*) to 0.31 (for *c*) under RCP-4.5 and 0.34 (for *scl*) to 0.45 (for *sic*) mm d^{-1} under RCP-8.5 (Fig. 5g and h). With regard to these results, it can be concluded that the finer-textured soils (i.e. *sicl*, *sic*, *cl* and *c*) showed a greater variation in changes of evaporation and transpiration with respect to the coarse-textured soils.

Although annual reference evapotranspiration (ET_0) is most likely to increase as a result of higher air temperature in the 2080s (Table 9), curtailed growth period would reduce ET_0 in the range of 0.034 (in Khorramabad) to 0.11 (in Sanandaj) under RCP-4.5

and 0.048 (in Khorramabad) to 0.20 (in Sanandaj) mm d^{-1} under RCP-8.5 averaged over all soils (Fig. 4f).

3.4.4. Runoff

Less water would run off in response to temperature rise and rainfall reduction (Zhang and Nearing, 2005) over the 2080s (Fig. 4g) particularly in those sites such as Kermanshah and Sanandaj which receive over 450 mm of precipitation (in the baseline). Averaged across all soils, the largest declines in runoff were 0.08 and 0.12 mm d^{-1} at Kermanshah under RCP 4.5 and 8.5, respectively. Surface runoff changes, averaged over the sites, ranged from −0.025 (in *sl*) to −0.061 (in *c*) under RCP-4.5 and from −0.034 (in *sl*) to −0.098 (in *c*) mm d^{-1} under RCP-8.5. Since runoff is a major component of finer-texture soils water balance, CC would cause a larger decrease of surface runoff in the fine-texture soils than in the coarse-texture ones during the growing season.

The box plots of changes in runoff for eight soils and sites in the 2080s relative to the baseline are depicted in Fig. 5i and j. The highest IQR values of ΔR were 0.29 and 0.28 mm d^{-1} for *c* under RCP-4.5 and RCP-8.5, respectively. There was a larger variation of ΔR (Fig. 5i and j) in the heavier-textured soils and wetter sites (i.e. Sanandaj, Khorramabad and Kermanshah).

3.4.5. Soil water storage changes

More water would be stored in soil profiles under most of the soil-climate simulation runs over the growing period (Fig. 4i). Offsetting reductions of E, D and R as well as shortened growth period seem to be likely causes of such increments in ΔS. The highest enhancement (mm d^{-1}) of ΔS, averaged over all stations, was predicted in *sicl* (by 0.032 under RCP-4.5 and 0.127 under RCP-8.5). In addition, a decrease in ΔS, averaged across all locations, was projected for *sl* (0.05 mm d^{-1}) and *scl* (0.03 mm d^{-1}) under RCP-4.5.

As a greater amount of water was projected to be withdrawn by crop root in the light-texture soils (i.e. *sl* and *scl*), a decrease (for RCP-4.5) or a slighter increase (for RCP-8.5) of ΔS is anticipated in such soils.

Furthermore, there was a significant variation in projected changes of ΔS (Fig. 5k and l). The greatest IQR of ΔS was simulated for *l* (0.19 mm d^{-1}) and *sil* (0.26 mm d^{-1}) under RCP-4.5 and RCP-8.5, respectively.

In conclusion, the results illustrated sensitivity of changes in yield and water balance components to soil texture under changing climate. The inherent uncertainties in this study arising from GCMs outputs, greenhouse gas emission pathways, applied downscaling technique and agrohydrological modeling should be taken into account by planners. It is worth noting that considering the daily change of components can partly, but not completely, reduce the effect of curtailed crop-growing season.

4. Conclusions

Our results indicate that yield loss, averaged over all soil textures, appears likely in Khorramabad, Khoy, Tabriz and Qazvin regions under both RCPs mainly due to NDJ rainfall shortage. Crop yield, averaged across all locations, is projected to decrease higher in the finer-textured soils. There would be a decline in runoff and drainage as a result of rainfall shortage during 2070–2099. Soil evaporation would likely decrease by 2100 due to soil water deficit, shortened growing season and changed ET partitioning. A higher decline of evaporation is anticipated in the coarser soils. Averaged over all soils, wheat would transpire less water at Tabriz, Khoy, Khorramabad and Qazvin regions as the consequence of drought (particularly during NDJ) and inappropriate sowing date. However, increased transpiration in some sites such as Nozheh and Sanandaj can be due to insignificant changes of NDJ rainfall, elevated CO_2 and more nitrogen availability resulted from decreased percolation. Averaged across all stations, higher increase of transpiration in sandy loam and sandy clay loam textures can be attributed to the larger amount of deeply stored water and the remarkable decline of N-leaching in such soils. The root zone water storage is predicted to increase under most of the soil-climate simulation runs particularly in the heavy-textured soils. The increment of root zone water storage seems to be smaller in the coarse-textured soils as a larger root water withdrawal is projected in such soils. Overall, diminished N-leaching in combination with higher deeply stored water in sandy loam and sandy clay loam textures would favor crop growth under CC. Meanwhile, we have shown that crop water budget and yield changes have a great sensitivity to soil texture under climatic changes. Taking soil physical variability into account can therefore result in more reliable projections and robust adaptation policy.

Acknowledgments

This research was financially supported by Tarbiat Modares University (TMU). The authors are deeply indebted to Iran Soil and Water Research Institute (SWRI) and Iran Meteorological Organization (IRIMO) for their collaboration in making required literature and data available. Authors also would like to thank Vali Feiziasl and Abdollali Ghafari from the Iranian Dryland Agricultural Research Institute (DARI) for providing some data and their worthwhile comments.

References

Asseng, S., Fillery, I., Dunin, F., Keating, B.A., Meinke, H., 2000. Potential deep drainage under wheat crops in a Mediterranean climate. I. Temporal and spatial variability. Crop Pasture Sci. 52, 45–56.

Bannayan, M., Eyshi Rezaei, E., 2014. Future production of rainfed wheat in Iran (Khorasan province): climate change scenario analysis. Mitig. Adapt. Strategies Glob. Change 19, 211–227.

Bannayan, M., Lakzian, A., Gorbanzadeh, N., Roshani, A., 2011. Variability of growing season indices in northeast of Iran. Theor. Appl. Climatol. 105, 485–494.

Bormann, H., 2012. Assessing the soil texture-specific sensitivity of simulated soil moisture to projected climate change by SVAT modelling. Geoderma 185, 73–83.

Cantelaube, P., Terres, J.-M., 2005. Seasonal weather forecasts for crop yield modelling in Europe. Tellus A 57, 476–487.

Chenoweth, J., Hadjinicolaou, P., Bruggeman, A., Lelieveld, J., Levin, Z., Lange, M.A., Xoplaki, E., Hadjikakou, M., 2011. Impact of climate change on the water resources of the eastern Mediterranean and Middle East region: modeled 21st century changes and implications. Water Resour. Res. 47.

Collins, M., Knutti, R., Arblaster, J., Dufresne, J.-L., Fichefet, T., Friedlingstein, P., Gao, X., Gutowski, W.J., Johns, T., Krinner, G., Shongwe, M., Tebaldi, C., Weaver, A., Wehner, M., 2013. Long-term climate change: projections, commitments and irreversibility. In: Stocker, T.F., Qin, D., Plattner, G.-K., Tignor, M.B.T., Allen, S.K., Boschung, J., Nauels, A., Xia, Y., Bex, V., Midgley, P.M. (Eds.), Climate Change 2013: the Physical Science Basis Contribution of Working Group I to the Fifth Assessment Report of the Intergovernmental Panel on Climate Change. Cambridge University Press, Cambridge, United Kingdom and New York, NY, USA, pp. 1029–1136.

Dai, A., 2011. Drought under global warming: a review. Wiley Interdiscip. Rev. Clim. Change 2, 45–65.

Dai, A., 2013. Increasing drought under global warming in observations and models. Nat. Clim. Change 3, 52–58.

Dettori, M., Cesaraccio, C., Motroni, A., Spano, D., Duce, P., 2011. Using CERES-Wheat to simulate durum wheat production and phenology in Southern Sardinia, Italy. Field Crops Res. 120, 179–188.

Donat, M.G., Leckebusch, G.C., Pinto, J.G., Ulbrich, U., 2010. European storminess and associated circulation weather types: future changes deduced from a multi-model ensemble of GCM simulations. Clim. Res. 42, 27–43.

Dufresne, J.-L., Foujols, M.-A., Denvil, S., Caubel, A., Marti, O., Aumont, O., Balkanski, Y., Bekki, S., Bellenger, H., Benshila, R., 2013. Climate change projections using the IPSL-CM5 earth system model: from CMIP3 to CMIP5. Clim. Dyn. 40, 2123–2165.

Dunne, J.P., John, J.G., Adcroft, A.J., Griffies, S.M., Hallberg, R.W., Shevliakova, E., Stouffer, R.J., Cooke, W., Dunne, K.A., Harrison, M.J., 2012. GFDL's ESM2 global coupled climate-carbon earth system models. Part I: physical formulation and baseline simulation characteristics. J. Clim. 25, 6646–6665.

Eitzinger, J., Štastná, M., Žalud, Z., Dubrovský, M., 2003. A simulation study of the effect of soil water balance and water stress on winter wheat production under different climate change scenarios. Agric. Water Manage. 61, 195–217.

Eitzinger, J., Trnka, M., Hösch, J., Žalud, Z., Dubrovský, M., 2004. Comparison of CERES, WOFOST and SWAP models in simulating soil water content during growing season under different soil conditions. Ecol. Model. 171, 223–246.
El Chami, D., Daccache, A., 2015. Assessing sustainability of winter wheat production under climate change scenarios in a humid climate—an integrated modelling framework. Agric. Syst. 140, 19–25.
Evans, J.P., 2009. 21st century climate change in the Middle East. Clim. Change 92, 417–432.
Eyshi Rezaie, E., Bannayan, M., 2012. Rainfed wheat yields under climate change in northeastern Iran. Meteorol. Appl. 19, 346–354.
Feiziasl, V., Toshieh, V., Esmaeilie, M., 2007. Study on the Effects of Different Sources and Rates of Soil Nitrogen on Quality and Quantities of Rain Fed Wheat. Ministry of Agriculture, Research and Education Organization. Dryland Agricultural Research Institute (DARI), Iran, pp. 148 (In persian).
Fernandez-Illescas, C.P., Porporato, A., Laio, F., Rodriguez-Iturbe, I., 2001. The ecohydrological role of soil texture in a water-limited ecosystem. Water Resour. Res. 37, 2863–2872.
Ferretti, D., Pendall, E., Morgan, J., Nelson, J., Lecain, D., Mosier, A., 2003. Partitioning evapotranspiration fluxes from a Colorado grassland using stable isotopes: seasonal variations and ecosystem implications of elevated atmospheric CO2. Plant Soil 254, 291–303.
Flato, G., Marotzke, J., Abiodun, B., Braconnot, P., Chou, S.C., Collins, W.J., Cox, P., Driouech, F., Emori, S., Eyring, V., 2013. Evaluation of climate models. In: Stocker, T.F., Qin, D., Plattner, G.-K., Tignor, M.B.T., Allen, S.K., Boschung, J., Nauels, A., Xia, Y., Bex, V., Midgley, P.M. (Eds.), Climate Change 2013: the Physical Science Basis. Contribution of Working Group I to the Fifth Assessment Report of the Intergovernmental Panel on Climate Change. Cambridge University Press, Cambridge, United Kingdom and New York, NY, USA, pp. 741–866.
Franks, S.W., 2002. Assessing hydrological change: deterministic general circulation models or spurious solar correlation? Hydrol. Process. 16, 559–564.
Fu, C., Wang, S., Xiong, Z., Gutowski, W.J., 2005. Regional climate model intercomparison project for Asia. Bull. Am. Meteorol. Soc. 86, 257.
Hatfield, J.L., Boote, K.J., Kimball, B., Ziska, L., Izaurralde, R.C., Ort, D., Thomson, A.M., Wolfe, D., 2011. Climate impacts on agriculture: implications for crop production. Agron. J. 103, 351–370.
He, Y., Hou, L., Wang, H., Hu, K., McConkey, B., 2014. A modelling approach to evaluate the long-term effect of soil texture on spring wheat productivity under a rain-fed condition. Sci. Rep. 4.
Hillel, D., 1998. Environmental Soil Physics: Fundamentals, Applications, and Environmental Considerations. Academic press, New York.
Homaee, M., Schmidhalter, U., 2008. Water integration by plants root under non-uniform soil salinity. Irrig. Sci. 27, 83–95.
Homaee, M., Dirksen, C., Feddes, R., 2002a. Simulation of root water uptake: I. Non-uniform transient salinity using different macroscopic reduction functions. Agric. Water Manage. 57, 89–109.
Homaee, M., Feddes, R., Dirksen, C., 2002b. A macroscopic water extraction model for nonuniform transient salinity and water stress. Soil Sci. Soc. Am. J. 66, 1764–1772.
Homaee, M., Feddes, R., Dirksen, C., 2002c. Simulation of root water uptake: II. Non-uniform transient water stress using different reduction functions. Agric. Water Manage. 57, 111–126.
Homaee, M., Feddes, R., Dirksen, C., 2002d. Simulation of root water uptake: III. Non-uniform transient combined salinity and water stress. Agric. Water Manage. 57, 127–144.
Hoogenboom, G., Jones, J.W., Wilkens, P.W., Porter, C.H., Boote, K.J., Hunt, L.A., Singh, U., Lizaso, J.I., White, J.W., Uryasev, O., Ogoshi, R., Koo, J., Shelia, V., Tsuji, G.Y., 2014. Decision Support System for Agrotechnology Transfer (DSSAT) Version 4.6. Washington, DSSAT Foundation Prosser www.DSSAT.net.
IPCC, 2013. Climate Change 2013: the Physical Science Basis. Contribution of Working Group I to the Fifth Assessment Report of the Intergovernmental Panel on Climate Change In: Stocker, T.F., Qin, D., Plattner, G.-K., Tignor, M.B.T., Allen, S.K., Boschung, J., Nauels, A., Xia, Y., Bex, V., Midgley, P.M. (Eds.),Cambridge University Press, Cambridge, United Kingdom and New York, NY, USA, p. 1535.
Jalota, S., Vashisht, B., Kaur, H., Kaur, S., Kaur, P., 2014. Location specific climate change scenario and its impact on rice and wheat in Central Indian Punjab. Agric. Syst. 131, 77–86.
Jones, P.G., Thornton, P.K., 2013. Generating downscaled weather data from a suite of climate models for agricultural modelling applications. Agric. Syst. 114, 1–5.
Jones, J.W., Hoogenboom, G., Porter, C.H., Boote, K.J., Batchelor, W.D., Hunt, L., Wilkens, P.W., Singh, U., Gijsman, A.J., Ritchie, J.T., 2003. The DSSAT cropping system model. Eur. J. Agron. 18, 235–265.
Kersebaum, K.C., Hecker, J.-M., Mirschel, W., Wegehenkel, M., 2007. Modelling water and nutrient dynamics in soil–crop systems: a comparison of simulation models applied on common data sets. In: Kersebaum, K.C. (Ed.), Modelling Water and Nutrient Dynamics in Soil–Crop Systems. Springer, pp. 1–17.
Lane, D.R., Coffin, D.P., Lauenroth, W.K., 1998. Effects of soil texture and precipitation on above-ground net primary productivity and vegetation structure across the Central Grassland region of the United States. J. Veg. Sci. 9, 239–250.
Lelieveld, J., Hadjinicolaou, P., Kostopoulou, E., Chenoweth, J., El Maayar, M., Giannakopoulos, C., Hannides, C., Lange, M., Tanarhte, M., Tyrlis, E., 2012. Climate change and impacts in the Eastern Mediterranean and the Middle East. Clim. Change 114, 667–687.
Li, Y., Ye, W., Wang, M., Yan, X., 2009. Climate change and drought: a risk assessment of crop-yield impacts. Clim. Res. 39, 31.
Ludwig, F., Asseng, S., 2006. Climate change impacts on wheat production in a Mediterranean environment in Western Australia. Agric. Syst. 90, 159–179.
Mearns, L.O., Rosenzweig, C., Goldberg, R., 1997. Mean and variance change in climate scenarios: methods, agricultural applications, and measures of uncertainty. Clim. Change 35, 367–396.
Muluneh, A., Biazin, B., Stroosnijder, L., Bewket, W., Keesstra, S., 2014. Impact of predicted changes in rainfall and atmospheric carbon dioxide on maize and wheat yields in the Central Rift Valley of Ethiopia. Reg. Environ. Change, 1–15.
Palosuo, T., Kersebaum, K.C., Angulo, C., Hlavinka, P., Moriondo, M., Olesen, J.E., Patil, R.H., Ruget, F., Rumbaur, C., Takáč, J., 2011. Simulation of winter wheat yield and its variability in different climates of Europe: a comparison of eight crop growth models. Eur. J. Agron. 35, 103–114.
Peel, M.C., Finlayson, B.L., McMahon, T.A., 2007. Updated world map of the Köppen-Geiger climate classification. Hydrol. Earth Syst. Sci. 11, 1633–1644.
Priestley, C., Taylor, R., 1972. On the assessment of surface heat flux and evaporation using large-scale parameters. Mon. Weather. Rev. 100, 81–92.
Rao, A.S., Shanker, A.K., Rao, V., Rao, V.N., Singh, A., Kumari, P., Singh, C., Verma, P.K., Kumar, P.V., Rao, B.B., 2015. Predicting irrigated and rainfed rice yield under projected climate change scenarios in the eastern region of India. Environ. Model. Assess., 1–14.
Rawls, W., Brakensiek, D., Saxton, K., 1982. Estimation of soil water properties. Trans. ASAE 25, 1316–1320.
Riahi, K., Rao, S., Krey, V., Cho, C., Chirkov, V., Fischer, G., Kindermann, G., Nakicenovic, N., Rafaj, P., 2011. RCP 8.5—a scenario of comparatively high greenhouse gas emissions. Clim. Change 109, 33–57.
Richardson, C.W., 1981. Stochastic simulation of daily precipitation, temperature, and solar radiation. Water Resour. Res. 17, 182–190.
Ritchie, J.T., 1972. Model for predicting evaporation from a row crop with incomplete cover. Water Resour. Res. 8, 1204–1213.
Ritchie, J.T., 1981. Water dynamics in the soil-plant-atmosphere system. Plant Soil 58, 81–96.
Ritchie, J.T., 1998. Soil water balance and plant water stress. In: Tsuji, G., Hoogenboom, G., Thornton, P. (Eds.), Understanding Options for Agricultural Production. Springer, Netherlands, pp. 41–54.
Ritchie, J.T., Porter, C.H., Judge, J., Jones, J.W., Suleiman, A.A., 2009. Extension of an existing model for soil water evaporation and redistribution under high water content conditions. Soil Sci. Soc. Am. J. 73, 792–801.
Rockström, J., Karlberg, L., Wani, S.P., Barron, J., Hatibu, N., Oweis, T., Bruggeman, A., Farahani, J., Qiang, Z., 2010. Managing water in rainfed agriculture—the need for a paradigm shift. Agric. Water Manage. 97, 543–550.
Rodríguez-Iturbe, I., Porporato, A., 2005. Ecohydrology of Water-Controlled Ecosystems: Soil Moisture and Plant Dynamics. Cambridge University Press, Cambridge, UK.
Saadat, S., Homaee, M., 2015. Modeling sorghum response to irrigation water salinity at early growth stage. Agric. Water Manage. 152, 119–124.
Sadeghi, A., Kamgar-Haghighi, A., Sepaskhah, A., Khalili, D., Zand-Parsa, S., 2002. Regional classification for dryland agriculture in southern Iran. J. Arid Environ. 50, 333–341.
Saxton, K., Rawls, W.J., Romberger, J., Papendick, R., 1986. Estimating generalized soil-water characteristics from texture. Soil Sci. Soc. Am. J. 50, 1031–1036.
Seneviratne, S.I., Corti, T., Davin, E.L., Hirschi, M., Jaeger, E.B., Lehner, I., Orlowsky, B., Teuling, A.J., 2010. Investigating soil moisture–climate interactions in a changing climate: a review. Earth Sci. Rev. 99, 125–161.
Song, Z., Qiao, F., Song, Y., 2012. Response of the equatorial basin-wide SST to non-breaking surface wave-induced mixing in a climate model: an amendment to tropical bias. J. Geophys. Res. Oceans 117, C00J26.
Suleiman, A.A., Ritchie, J.T., 2004. Modifications to the DSSAT vertical drainage model for more accurate soil water dynamics estimation. Soil Sci. 169, 745–757.
Tabari, H., Talaee, P.H., 2011a. Analysis of trends in temperature data in arid and semi-arid regions of Iran. Global Planet. Change 79, 1–10.
Tabari, H., Talaee, P.H., 2011b. Temporal variability of precipitation over Iran: 1966–2005. J. Hydrol. 396, 313–320.
Tabari, H., Shifteh Somee, B., Rezaeian Zadeh, M., 2011. Testing for long-term trends in climatic variables in Iran. Atmos. Res. 100, 132–140.
Tai, A.P.K., Martin, M.V., Heald, C.L., 2014. Threat to future global food security from climate change and ozone air pollution. Nat. Clim. Change 4, 817–821.
Talaee, P.H., Some'e, B.S., Ardakani, S.S., 2014. Time trend and change point of reference evapotranspiration over Iran. Theor. Appl. Climatol. 116, 639–647.
Tebaldi, C., Knutti, R., 2007. The use of the multi-model ensemble in probabilistic climate projections. Philos. Trans. R. Soc. Lond. Ser. A 365, 2053–2075.
Thomson, A.M., Calvin, K.V., Smith, S.J., Kyle, G.P., Volke, A., Patel, P., Delgado-Arias, S., Bond-Lamberty, B., Wise, M.A., Clarke, L.E., 2011. RCP4. 5: a pathway for stabilization of radiative forcing by 2100. Clim. Change 109, 77–94.
Thornton, P.K., Jones, P.G., Alagarswamy, G., Andresen, J., 2009. Spatial variation of crop yield response to climate change in East Africa. Global Environ. Change 19, 54–65.
Tseng, H.-W., Gan, T.Y., Yu, P.-S., 2015. Composite drought indices of monotonic behaviour for assessing potential impact of climate change to a water resources system. Water Resour. Manage. 29, 2341–2359.
Tubiello, F.N., Rosenzweig, C., Volk, T., 1995. Interactions of CO_2, temperature and management practices: simulations with a modified version of CERES-Wheat. Agric. Syst. 49, 135–152.

UNEP, 1992. World Atlas of Desertification. United Nations Environment Programme, London.
Watanabe, S., Hajima, T., Sudo, K., Nagashima, T., Takemura, T., Okajima, H., Nozawa, T., Kawase, H., Abe, M., Yokohata, T., 2011. MIROC-ESM 2010: model description and basic results of CMIP5-20c3 m experiments. Geosci. Model Dev. 4, 845–872, http://dx.doi.org/10.5194/gmd-4-845-2011.
Williams, J., Jones, C., Dyke, P., 1984. Modeling approach to determining the relationship between erosion and soil productivity. Trans. ASAE 27.
Willmott, C.J., Robeson, S.M., Matsuura, K., 2012. A refined index of model performance. Int. J. Climatol. 32, 2088–2094.
Wu, T., 2012. A mass-flux cumulus parameterization scheme for large-scale models: description and test with observations. Clim. Dyn. 38, 725–744.
Yang, Y., Li Liu, D., Anwar, M.R., Zuo, H., Yang, Y., 2014. Impact of future climate change on wheat production in relation to plant-available water capacity in a semiarid environment. Theor. Appl. Climatol. 115, 391–410.
Yang, Y., Li Liu, D., Anwar, M.R., O'Leary, G., Macadam, I., Yang, Y., 2015. Water use efficiency and crop water balance of rainfed wheat in a semi-arid environment: sensitivity of future changes to projected climate changes and soil type. Theor. Appl. Climatol., 1–15.
Zhang, X., Nearing, M., 2005. Impact of climate change on soil erosion, runoff, and wheat productivity in central Oklahoma. Catena 61, 185–195.
van Ittersum, M., Howden, S., Asseng, S., 2003. Sensitivity of productivity and deep drainage of wheat cropping systems in a Mediterranean environment to changes in CO_2 temperature and precipitation. Agric. Ecosyst. Environ. 97, 255–273.